THE MICROWAVE STRUCTURE OF CORONAL CONDENSATIONS AND ITS RELATION TO PROTON FLARES

HARUO TANAKA and SHINZO ÉNOMÉ

The Research Institute of Atmospherics, Nagoya University, Japan

(Received 4 October 1973; in revised form 29 October, 1974)

Abstract. Active regions on the Sun in the 20th solar cycle are studied with special reference to their association with proton flares based on microwave interferometric observations at Toyokawa Observatory. It has been reconfirmed that the active regions associated with intense *S*-component emission with a high 3-cm to 8-cm flux ratio are likely to produce proton flares.

About one fourth of 259 active regions during the period investigated are found to have definite features in the spatial distribution of polarization at a wavelength of 3 cm. Active regions with one particular type of polarization pattern have a good correlation with the occurrence of proton flares.

1. Introduction

Whether or not a certain active region on the solar disk will generate a solar flare within a specific period of time may be one of the most frequently asked questions of solar physicists or astronomers. For those specialists, on the other hand, this question may correspond to a study of what characteristics those active regions which produce important flares or proton flares have in common. The prediction or forecast of solar flares is an application of the study of flare activity or flare productivity.

The recent status of studies and applications on this subject has been described in some detail by Severny and Steshenko (1972) and Pick and Simon (1973). As pointed out by Severny and Steshenko, there have been two viewpoints in the study of flare generation in solar active regions. One is to investigate the special characteristics of those active regions which yield important or proton flares; high gradient of longitudinal fields, bifurcated transverse fields, A-configurations, δ-configurations, and so on. Another viewpoint is to trace evolutionary features of active regions producing important or proton flares; for example, it has already been well established by many workers that the birth of a spot group in or near an old region leads to a complex evolution of the group favorable for producing proton flares (Bruzek, 1972).

Besides these two viewpoints, there may be a different aspect of the study relating to the height in the solar atmosphere, that is to say, investigating what physical quantities at what level in the solar atmosphere are really useful for the flare prediction. Most information is obtained by photospheric observations such as magnetic and velocity fields, sunspot configurations, etc. As coronal parameters, X-ray and radio observations have been utilized to investigate correlations between the occurrence of type IV, PCA or proton flares and spectral and spatial features of those radiations from active regions (Kundu, 1959; Pick, 1961; Michard and Ribes, 1968; Tanaka and Kakinuma, 1964). Though radio methods of investigation have a defect in that the spatial resolution is not sufficient for detailed analysis, they give information that has a very significant physical meaning, since enhanced dm- and cm-radio emissions are radiated from coronal condensations permeated by strong sunspot magnetic fields of say 1000 G, where solar flare instabilities may be generated and/or amplified.

In the present paper, we shall study spatial and polarization features of the radio emission of active regions in the 20th solar cycle referring to their productivity of proton flares. The resolution of our interferometers has been improved to 1.1′ from 2.2′ or 4.5′ in the previous study (Tanaka and Kakinuma, 1964).

2. Analysis of Data

We have selected 259 active regions during the period from 1967 through 1971, each associated with *S*-components larger than 5 solar flux unit (10^{-22} Wm^{-2} Hz^{-1}) at a wavelength of 3 cm. Those active regions have been listed in the form as shown in Table I, where only selected regions are listed due to limitation of space. In this table, McMath numbers are used for identification. Other parameters which characterize the active regions are heliographic latitude, CMP date, 3-cm flux, 3-cm to 8-cm flux ratio (old calibration is used here; factors 1.08 and 1.15 should be multiplied for flux and flux ratio respectively to convert to absolute values used in URSIGRAM from 1974), and the type of spatial distribution of the region's 3-cm polarization which will be explained later in detail. In the final three columns are shown the dates of associated great bursts (10-cm flux greater than 500 sfu), proton events, and relativistic electron events. In selecting solar proton events, reference is made to the measurements on

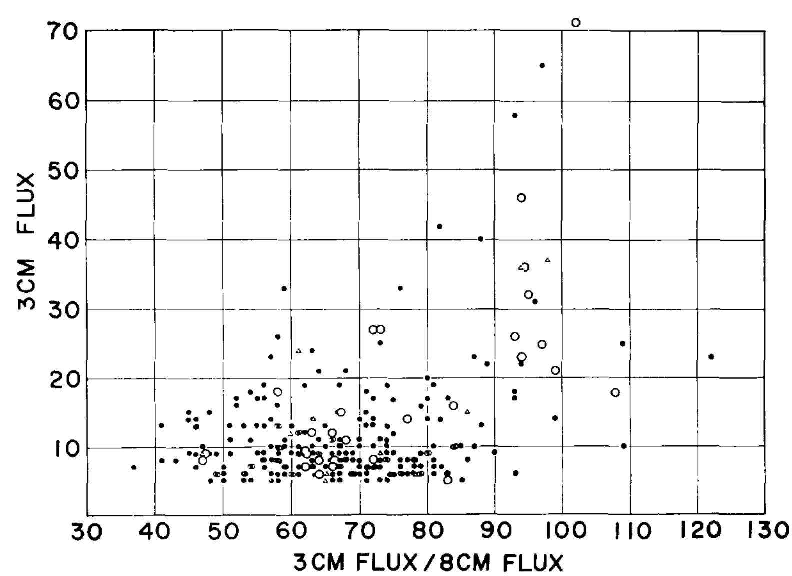

Fig. 1. Diagram of 3-cm flux vs 3-cm to 8-cm flux ratio for 259 active regions during four years from 1968 to 1971. Open circles, triangles, and filled circles correspond to proton centers, active regions associated with an energetic particle event above 10 MeV, and non-proton centers, respectively.

TABLE I

Characteristics of the selected 28 well-isolated active regions with 3-cm flux ⩾ 10 and 3-cm/8-cm flux ratio ⩾ 0.8. In the sixth column, radio polarization features are classified according to the P-, E- and S-configuration system. In the final three columns, dates of 10-cm bursts, proton events and relativistic electron events are given. Dates for weak proton events in the 10 MeV range and for radio bursts smaller than 500 sfu are parenthesized

McMath region	Latitude	CMP date	3-cm flux	Flux ratio	Radio pol.	10-cm burst	Proton event	Relat. electron event
		1967						
9128	S 19	Dec 28	23	87	S			
		1968						
9153	N 20	Jan 13	19	81	S			
9184	N 14	Jan 31	65	97	E	(Feb 2)		
9188	N 17	Feb 3	14	99	S			
9273	S 16	Mar 24	14	80	S			Mar 30
9131	N 22	Apr 15	22	89	S			
9503	N 12	Jul 13	32	95	S	Jul 6	Jul 6	Jul 6
						Jul 8	Jul 9	
9567	N 13	Aug 8	23	94	P	Aug 3	(Aug 5)	
						Aug 14	Aug 14	
9593	S 17	Aug 18	20	80	S			
9740	S 15	Oct 28	46	94	S	(Oct 26)	(Oct 26)	
9826	S 16	Dec 22	17	93	S			
		1969						
9946	N 18	Feb 23	18	108	P	Feb 24	(Feb 25)	
						Feb 25	Feb 25	Feb 25
						Feb 26	Feb 26	
						Feb 27	Feb 27	Feb 27
[9994	N 18	Mar 18	10	81				
[9994	N 22	Mar 21	36	94	P	Mar 21	Mar 21	
						Mar 21		
						Mar 27	(Mar 27)	
						Mar 30	Mar 30	Mar 30
10014	N 15	Apr 3	42	82	S			
10181	S 16	Jul 7	22	94	S			
10385	N 12	Oct 26	25	97	S	Nov 2	Nov 2	
10432	N 10	Nov 22	71	102	S	Nov 18		
						Nov 24	Nov 24	
10449	S 15	Dec 1	14	82	S			
		1970						
10568	N 16	Feb 10	31	96	E	Feb 11		
10581	S 23	Feb 19	18	93	S			
10669	S 14	Apr 9	42	80	E	(Apr 6)	(Apr 7)	
10789	N 19	Jan 17	37	98	P	Jun 14	(Jun 14)	
10812	S 13	Jul 4	26	93	S	Jul 4	Jul 7	
10845	N 13	Jul 24	21	99	S	Jul 20	(Jul 21)	
						Jul 22	Jul 23	
						Jul 23	Jul 24	
10865	N 18	Aug 9	25	109	S			
11029	N 15	Nov 14	40	88	E	Nov 16		
		1971						
11134	S 12	Jan 30	17	83	S			
11610	S 13	Nov 19	23	122	S			

board Explorers 34 and 41 listed in *Solar Geophysical Data*, NOAA. The adopted threshold of the integrated flux for the proton event is 10^6 protons cm^{-2} above 30 MeV, which is expected to be consistent with that of the previous study. Electron events are referred to the observations by OGO-5 and IMP-4 (Datlowe, 1971; Simnett, 1972).

The 3-cm flux and 3-cm to 8-cm flux ratio of the *S*-component have been found to be good indicators of the productivity of solar proton flares in the active region (Tanaka and Kakinuma, 1964). These relations for the current solar cycle may be seen in Figure 1, where all the active regions in the original table are plotted on a 3-cm flux vs flux ratio diagram. Open circles represent those regions which were associated with proton flares (proton centers) and filled circles are those not associated with proton flares (non-proton centers). Triangles correspond to those regions which were associated with particle events in the 10 MeV range. These 10 MeV events may be identified as energetic storm particle events (Obayashi, 1966) or delayed events (Lin *et al.*, 1968; McCracken and Rao, 1970).

There were 29 proton centers during the period investigated, which are distributed very sparsely and rather homogeneously in the flux vs flux ratio diagram of Figure 1. This fact suggests that proton centers do not tightly correlate with the 3-cm flux nor the flux ratio. In other words, some proton flares, though not many, are produced in active regions which are of minor importance in the microwave range. A typical example is the proton flare of November 5th, 1970. It occurred in the active region McMath 11019, which was associated with an *S*-component of 8 sfu at 3 cm and with a 0.47 flux ratio. The sunspot area of this region was 50 millionths of the solar hemisphere.

However, if we take the ratio of the number of proton centers to that of all active regions in a certain restricted domain in Figure 1, the ratio is found to increase as we move along the horizontal axis away from the vertical one, or along the vertical axis away from the horizontal one. The number ratios of proton centers to all active regions are 9/33 and 8/23 for the domains where the 3-cm flux is larger than 20 sfu and where the flux ratio is greater than 0.9, respectively. This trend generally agrees with the results of the previous solar cycle (Kundu, 1959; Pick, 1961; Tanaka and Kakinuma, 1964). Although, it is obvious that both the 3-cm flux and the flux ratio of the *S*-component for active regions in the current solar cycle are generally much smaller than those in the previous solar cycle, it is, however, also evident that there were several powerful active regions in this cycle, each of which produced a ground level event (GLE) and/or two or three proton flares. Examples of such powerful regions are McMath 9740, 9946 and 9994. It is remarkable that these powerful active regions were always associated with strong *S*-components of large flux and high flux ratio. This means that, although these powerful active regions are very few in one solar cycle, we might still be able to expect a proton flare when a strong *S*-component appears on the solar disk. This statement is equivalent to the conclusion of our previous study in the 19th solar cycle (Tanaka and Kakinuma, 1964).

The occurrence probability and the number ratio of proton centers to all active regions are 17/42 and 8/42, respectively, for those active regions associated both with S-components greater than 10 sfu at 3 cm and with flux ratios greater than 0.8. These figures, however, are found to be much smaller than those in the 19th solar cycle. Possible explanations for this difference may be among the following:

(i) The criterion for proton flares may be to some extent more severe than that in the previous solar cycle.

(ii) The nature of activity may have changed.

(iii) The improvement in the spatial resolution of our radio observations may have introduced a higher possibility of picking up those active regions with small S-component emissions.

Among these possibilities, (iii) is considered to be the most serious, so that it may be almost impossible to say how much difference there was between the solar activity in the current and previous solar cycles.

Although the improvement in resolution might have led to the loss of homogeneity in the data over the two solar cycles, it enabled us to resolve active regions and provided us information on the spatial structure of coronal condensations.

About one fourth of the active regions for the period investigated had definite features in the distribution of brightness and polarization across the coronal condensations. These features have been classified into three groups. Each group has a distinct pattern of polarization distribution at 3 cm wavelength. We shall call these patterns P, E and S configurations. Examples of these configurations are shown in Figure 2.

The P-configuration is characterized by a strongly polarized main peak with oppositely polarized sub-peaks on either side. Typical separation of the peaks is 1′ or less. The E-configuration consists of two oppositely polarized peaks with roughly equal degrees of polarization. The separation of these two peaks is usually around 2′. Lastly, the S-configuration appears to be made up of a strongly polarized single peak.

The interpretation of the spectrum and polarization of S-components has been well established (Zheleznyakov, 1962; Kakinuma and Swarup, 1962). Typical brightness

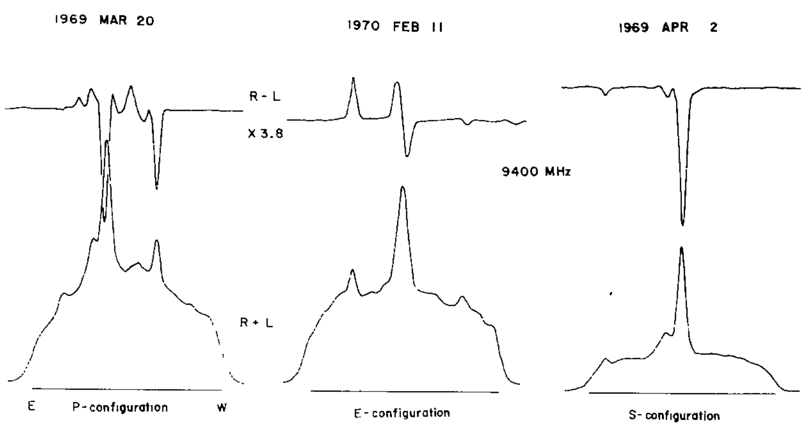

Fig. 2. Strip-scan curves of the Sun in intensity ($R+L$) and polarization ($R-L$) at a wavelength of 3 cm showing examples of P-, E- and S-configurations.

temperatures for these coronal condensations are 3×10^6 K at 8 cm and 5×10^5 K at 3 cm. The degree of polarization is low at 8 cm ($<5\%$) and high at 3 cm ($\leqslant 30\%$). These facts imply that (a) the condensation is optically thick at 8 cm and thin at 3 cm, (b) a field of 450 G permeates the major part of these coronal condensations where the temperature is 3×10^6 K, and (c) the temperature is 5×10^5–10^6 K and the field strength is 1200 G at the lower part of them. Radio polarization is correlated with magnetic polarity such that right-handed circular polarization corresponds to north (positive) magnetic polarity and left-handed corresponds to south polarity. The existence of three patterns of polarization distribution (P, E and S) suggests that corresponding magnetic field distributions occur in coronal condensations. In the following we shall examine the relation between proton centers and these three distinct patterns of polarization.

From the 42 major active regions described above (3-cm flux $\geqslant 10$, 3-cm/8-cm flux ratio$\geqslant 0.8$), we have selected 28 'well-isolated' regions as shown in Table I, and grouped them according to our P, E, and S classification. The result is shown in Table II. Among four P-configuration active regions, three were proton centers and

TABLE II

Association of the polarization classification with proton events for strong active regions. Weak event means weak proton event in the 10 MeV range not reaching the threshold of defined proton event, i.e., integrated flux of 10^6 protons cm^{-2} above 30 MeV

	Proton event	Weak event	No protons	Total
P-configuration	3	1		4
E-configuration		4		4
S-configuration	5	1	14	20
Total	8	6	14	28

one produced a delayed or weak event. On the other hand, the four E-configuration active regions were not proton centers. It should be pointed out, however, that those active regions did yield microwave bursts with intensities ranging from a few hundreds to a few thousands sfu, though they were not associated with solar proton emission with energies greater than 30 MeV. In particular, radio bursts on February 11, 1970 and November 16, 1970 did not accompany a delayed nor a weak event, although the associated flares were located at favorable heliographic positions for the propagation of solar protons through interplanetary space. Finally, twenty S-configuration active regions are classified into five proton centers, fourteen no-proton centers, and one delayed or weak event source.

Although the number of selected regions is not large, the above result suggests a good correlation between P-configuration active regions and proton centers. If we take all 259 regions in the original table, they can be classified as shown in Table III. This table also indicates that the occurrence of a proton flare is most probable in the P-configuration active region.

TABLE III

Numbers of active regions classified according to 3-cm polarization features that were associated with proton flares, weak proton events, and microwave bursts

	Active region	Proton event	Weak event	10-cm burst
P-configuration	6	8	4	12
E-configuration	26	3	3	11
S-configuration	53	17	9	27
Unpolarized	174	12	6	16
Total	259	40	22	66

3. Discussions

It is instructive to compare the patterns of polarization distribution with photospheric and chromospheric features, although the resolution of the radio observations is of course not as good as the optical measurements. Comparison of radio strip-scan curve with Mt. Wilson magnetograms has revealed good resemblance in general features, for example, Figure 3 shows the sunspot drawing and Mt. Wilson magnetograms of active region McMath 9994 taken from *Solar Geophysical Data*, NOAA. The corresponding radio drift curves of the P-configuration region are shown on the left-hand side in Figure 2. This active region was formed with two pairs of bipolar groups very close to each other. It is to be noticed that the central two narrowly-separated sunspots, namely the following spot in the preceding group and the preceding spot in the following group, were at a well developed stage of evolution. It is remarkable that if one looks only at this portion of the region, the ordering of the spots was reverse to the

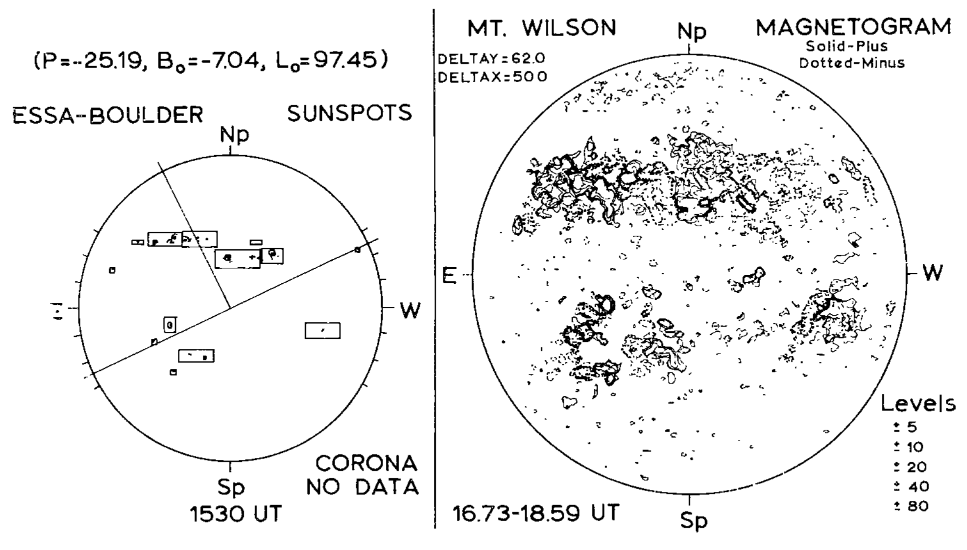

Fig. 3. Sunspot drawing and Mt. Wilson magnetogram on March 20, 1969, from *Solar Geophysical Data*, NOAA.

normal polarity law. Sunspot configurations like this may correspond to the reversed polarity regions identified by Smith and Howard (1968), who have shown their close relationship with the occurrence of importance 3 flares.

Sunspot sketches and magnetograms of the E-configuration active regions in our study show bipolar groups which are not typical, in the sense that the following spot was well developed and as big as the preceding spot.

In the case of S-configuration regions, sunspots are mostly α-type and their appearance is compact and simple, whereas some regions associated with proton flares are compact but complex. The latter suggests the existence of finer spatial structure in the microwave emission which may be revealed if the resolving power will be further improved.

The analysis made so far suggests a possible form of magnetic field lines in the P-configuration coronal condensation which is very similar to that of the X-type neutral sheet model developed by Sweet (1956), Petschek (1964) and Syrovatskii (1966). On the other hand, a suggested form of field lines in the E-configuration regions, which are mostly correlated with sub-relativistic electron or minor proton events, may correspond to the current limitation model by Alfvén and Carlquist (1967).

Finally, in order to demonstrate the effectiveness of the P, E and S classification

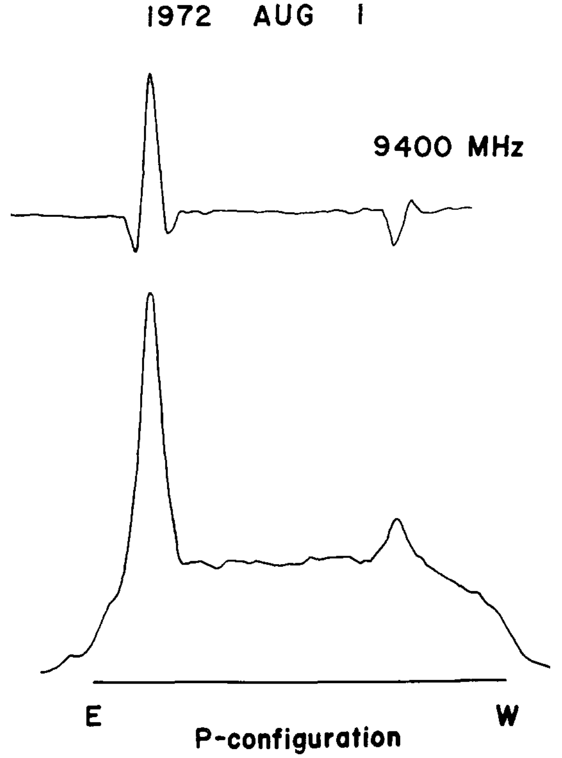

Fig. 4. Strip-scan curves of the Sun in intensity (bottom) and polarization (top) at a wavelength of 3 cm on August 1, 1972.

system, we illustrate in Figure 4 the brightness and polarization distribution of active region McMath 11976, which produced a series of large proton flares in August 1972.

4. Conclusion

Radio analysis of 259 active regions in the 20th solar cycle has revealed that

(1) proton centers are distributed rather homogeneously in a 3-cm flux vs 3-cm to 8-cm flux ratio diagram;

(2) the occurrence probability of proton events, however, is higher for those active regions with intense 3-cm flux and high flux ratio;

(3) for one fourth of the active regions studied, the shape of the polarization distribution across the coronal condensation can be classified into three definite groups called P-, E- and S-configurations;

(4) p-configuration regions are found to be closely associated with proton centers and proton events;

(5) in the E-configuration regions, electrons and protons are accelerated to sub-relativistic and less than MeV energies, respectively.

References

Alfvén, H. and Carlqvist, P.: 1967, *Solar Phys.* **1**, 220.
Bruzek, A.: 1972, in C. de Jager (ed.), *Solar-Terrestrial Physics*/1970, Part I, 49.
Datlowe, D.: 1971, *Solar Phys.* **17**, 436.
Gopasyuk, S., Ogir, M., Severny, A. B., and Shposhnikova, E.: 1963, *Izv. Krymsk. Astrofiz. Obs.* **29**, 15.
Kakinuma, T. and Swarup, G.: 1962, *Astrophys. J.* **136**, 975.
Kundu, M. R.: 1959, *Ann. Astrophys.* **22**, 1.
Lin, R. P., Kahler, S. W., and Roelof, E. C.: 1968, *Solar Phys.* **4**, 338.
McCracken, K. G. and Rao, U. R.: 1970, *Space Sci. Rev.* **11**, 155.
Michard, R. and Ribes, E.: 1968, in K. O. Kiepenheuer (ed.), 'Structure and Development of Solar Active Regions', *IAU Symp.* **35**, 420.
Obayashi, T.: 1966, *Rep. Ionosph. Space Res. Japan* **20**, 3.
Petschek, H. E.: 1964, Proc. AAS-NASA Symp. Physics of Solar Flares, NASA SP-50, 415.
Pick, M.: 1961, *Ann. Astrophys.* **24**, 183.
Pick, M. and Simon, P.: 1973, *Proc. IEEE* **61**, 1303.
Severny, A. B. and Steshenko, N. V.: 1972, in C. de Jager (ed.), *Solar Terrestrial Physics/1970*, Part I, 173.
Simnett, G. M.: 1972, *Solar Phys.* **22**, 189.
Smith, S. F. and Howard, R.: 1968, in K. O. Kiepenheuer (ed.), Structure and Development of Solar Active Regions', *IAU Symp.* **35**, 33.
Sweet, P. A.: 1956, in B. Lehnert (ed.), 'Electromagnetic Phenomena in Cosmical Physics', *IAU Symp.* **6**, 123.
Syrovatskii, S. I.: 1966, *Soviet Astron. – AJ* **10**, 270.
Tanaka, H. and Kakinuma, T.: 1964, *Rep. Ionosph. Space Res. Japan* **18**, 32.
Zheleznyakov, V. V.: 1962, *Soviet Astron. – AJ* **6**, 3.